ADVANCED FUNCTIONAL MATERIALS
www.afm-journal.de



# Ordering of Disordered Nanowires: Spontaneous Formation of Highly Aligned, Ultralong Ag Nanowire Films at Oil–Water–Air Interface

By *Hong-Yan Shi, Bo Hu, Xiao-Chun Yu, Rong-Li Zhao, Xi-Feng Ren, Shi-Lin Liu, Jian-Wei Liu, Mei Feng, An-Wu Xu,* and *Shu-Hong Yu**

**One-dimensional nanomaterials and their assemblies attract considerable scientific interest in the physical, chemical, and biological fields because of their potential applications in electronic and optical devices. The interface-assembly method has become an important route for the self-assembly of nanoparticles, nanosheets, nanotubes, and nanorods, but the self-assembly of ultralong nanowires has only been successful using the Langmuir–Blodgett approach. A novel approach for the spontaneous formation of highly aligned, ultralong Ag nanowire films at the oil–water–air interface is described. In this approach, the three-phase interface directs the movement and self-assembly process of the ultralong Ag nanowires without the effect of an external force or complex apparatus. The ordered films exhibit intrinsic large electromagnetic fields that are localized in the interstitials between adjacent nanowires. This new three-phase-interface approach is proven to be a general route that can be extended to self-assemble other ultralong nanowires and produce ordered films.**

## 1. Introduction

The synthesis of one-dimensional nanomaterials has achieved great success with the development of synthetic methodologies.[1] From the viewpoint of applications, one of the most difficult problems has been how to assemble these nanomaterials into functional nanomaterials and nanodevices. Discovering new methods to assemble one-dimensional nanomaterials into two- or three-dimensional structures has attracted lots of attention, owing to the potential applications in electronic and optical devices.[2–6]

Interfacial assembly, a very simple and effective approach, without complex installation, has become a hot area of research in recent years. The self-assembly of nanomaterials at the liquid–liquid interface has achieved great success, especially the self-assembly of nanoparticles,[7–9] nanosheets,[10] nanotubes,[6] and nanorods.[11] The main driving force for the assembly of nanoparticles at the liquid–liquid interface generally involves the decrease of the interfacial energy,[10,12] electrostatic forces,[13,14] and the interaction between capping molecules.[15] The self-assembly of colloids at the water–air interface is a mature technique for the fabrication of three-dimensional photonic band-gap crystals.[16] Furthermore, self-assembly at the substrate–solution–air interface has been investigated for the self-assembly of carbon nanotubes[4] and gold nanorods.[3] Although most of these methods have been successful in the assembly of nanoparticles, nanorods, nanotubes and nanoplates, few reports have been implemented as to the assembly of nanowires with high aspect ratios into highly aligned structures, based on their intrinsic properties at the interface.

The effect of the nanomaterial geometry has a great influence on the self-assembly process. Israelachvili et al.[14] reported that the magnitude and range of the repulsive forces for wires, rods, and particles decrease in sequence. For this reason, many techniques have been designed for the self-assembly of nanoparticles,[17,18] but only the Langmuir–Blodgett (LB) approach has successfully assembled nanowires.[5,19] Yang et al.[5,20] reported that assembly monolayers of aligned silver nanowires could be obtained via the LB technique. Silver nanowires were dispersed on the surface of water due to the interactions between surfactants and the nanowires, and they were compressed to a higher density on the surface by increasing the surface pressure, which caused the nanowires to reorient themselves and align parallel to each other. The LB technique, however, usually needs special equipment and has a complex operating process. The surfaces of the nanowires also need to be capped with hydrophobic molecules in order to make them float on the surface of water.

[*] Prof. S. H. Yu, H. Y. Shi, B. Hu, J. W. Liu, M. Feng, A. W. Xu
Division of Nanomaterials and Chemistry
Hefei National Laboratory for Physical Sciences at Microscale
Department of Chemistry
University of Science and Technology of China
Hefei, Anhui 230026 (PR China)
E-mail: shyu@ustc.edu.cn
Prof. S. L. Liu, X. C. Yu, R. L. Zhao
Department of Chemical Physics
University of Science and Technology of China
Hefei, Anhui 230026 (PR China)
Dr. X. F. Ren
Key Laboratory of Quantum Information
University of Science and Technology of China
Hefei, Anhui 230026 (PR China)

DOI: 10.1002/adfm.200901668

In this paper, we describe a new route for the self-assembly of hydrophilic Ag nanowires with a high aspect ratio, at the oil–water–air interface: different to previous reports on assembly at a two-phase interface, the films here are assembled at this three-phase interface. In these experiments, no two-phase interface of the three different phases can achieve the assembly of Ag nanowires. When an appropriate amount of an aqueous dispersion of Ag nanowires was dropped onto the surface of chloroform, the water–oil-air interface could be formed. The formation of a three-phase interface is necessary for the movement and self-assembly of ultralong Ag nanowires. Using this facile approach, Ag nanowires with a high aspect ratio were close-packed and aligned parallel to each other. The resulting, dry, freestanding films could grow as large as several square centimeters. Polarized UV-vis spectroscopy and surface-enhanced Raman spectroscopy (SERS) demonstrated that large electromagnetic (EM) fields were localized in the interstitials between adjacent Ag nanowires. It has been found that other ultralong nanomaterials, such as $Ag_6Mo_{10}O_{33}$ and Te nanowires, and $Bi_2S_3$ nanoribbons, can also be self-assembled using this new three-phase interface approach.

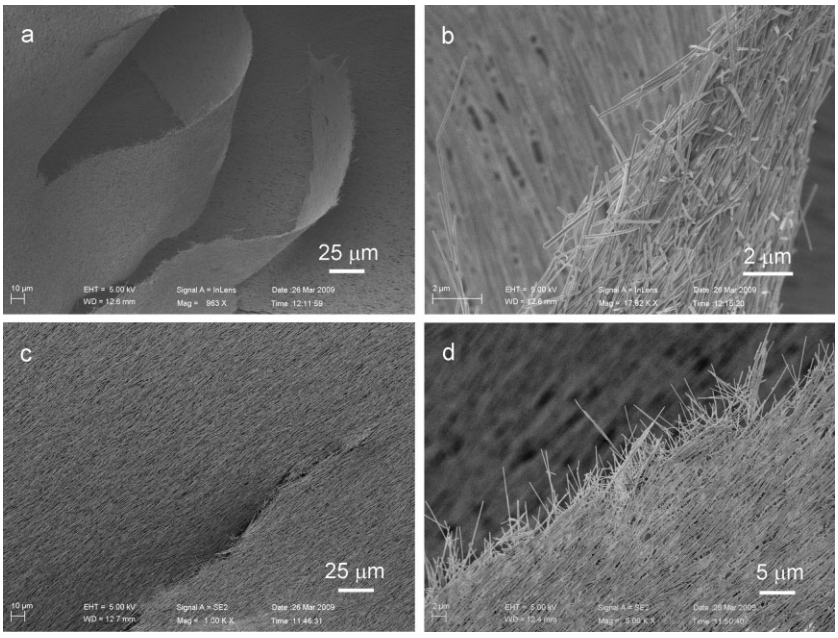


**Figure 2.** Low- and high-magnification SEM images of freestanding dry films of the Ag nanowires.

## 2. Results and Discussion

Firstly, we synthesized uniform, hydrophilic Ag nanowires with a high aspect ratio, which were 80–100 nm in diameter and 20–30 μm in length (Fig. 1a). A high-resolution transmission electron microscopy (HRTEM) image and the corresponding selected-area electron diffraction (SAED) pattern of a single Ag nanowire showed that it was well-crystalline with its surface being enclosed by both {100} and {111} facets (see Supplementary Information, Fig. S1). The Ag nanowires were then assembled using the novel three-phase-interface approach. A sparkling film appeared on the water surface, showing that the Ag nanowires had been successfully assembled in this process. The film could be transferred to a conveniently hydrophilic substrate, such as a glass or silicon wafer.

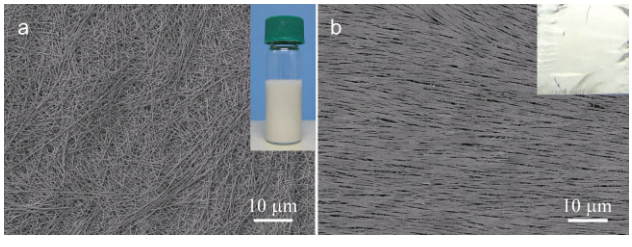


**Figure 1.** a) SEM image of the disordered Ag nanowires and an optical photograph of them dispersed in distilled water. b) SEM image of the assembly nanowires and an optical photograph of the nanowires transferred onto a silicon wafer.

A typical SEM image of the film reveals that a number of the Ag nanowires were assembled parallel to each other and aligned side-by-side over a large area (Fig. 1, and Supplementary Information, Fig. S2). The optical photograph of the film, which had been transferred from the water surface to a silicon wafer, showed a similar luster of the film as a silver mirror. Interestingly, this three-phase-interface approach could thoroughly implement the self-assembly of the Ag nanowires, and effectively prevent the interfusion of the Ag nanoparticles that are the by-products of the synthesis of Ag nanowires. The X-ray diffraction (XRD) pattern of the silver nanowires and the film has demonstrated this point, because of the sharp decrease in intensity of the characteristic peaks (220) and (311) that were just able to be observed from the Ag nanoparticles (see Supplementary Information, Fig. S1b). After drying in ambient conditions for one day, the dry, freestanding films could be fully desquamated from the substrate by immersing the substrate in water. Scanning electron microscopy (SEM) images of a freestanding film on a copper loop demonstrated the close-packed states of the Ag nanowires (Fig. 2).

The formation of the film through this three-phase-interface approach is proposed as shown in Scheme 1. Initially, the three phases of the oil–water–air interface were formed by dropping an appropriate amount of an aqueous solution of the Ag nanowires onto the surface of chloroform. In the first step, the Ag nanowires transferred step-by-step from the water–oil interface to the water–air interface through the oil–water–air interface line. In the second step, the Ag nanowires at the water–air interface self-assembled, initially at the contact line of the wall of the beaker and the water phase, which can be denoted as the water–air-substrate interface. In the third step, the film of the Ag nanowires at the water–air-substrate interface grew into a continuous film. Finally, the film of Ag nanowires covered the whole water–air interface.

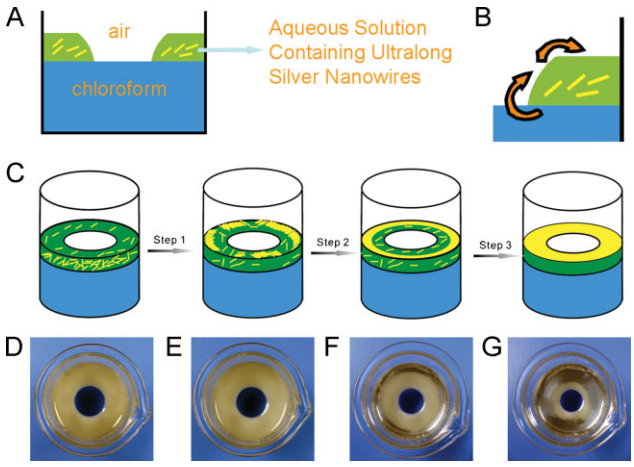


**Scheme 1.** A) The cross-section of the three-phase interface. B) Schematic illustration of the movement of the Ag nanowires in the first step with the evaporation of the oil phase. C) Schematic representation of the stages of film formation of the Ag nanowires at the three-phase interface. D–G) The corresponding experimental optical images of the steps shown in Scheme 1C.

In contrast, a two-phase interface cannot achieve the self-assembly of Ag nanowires (see Supplementary Information, Fig. S3). When excessive aqueous solution of the Ag nanowires was rapidly added to the chloroform surface, covering the whole surface, two interfaces were formed, including the air-water interface and the oil–water interface. No film could be observed on the water–air interface after the solution had been standing for a long time, which indicates that the assembly cannot be achieved at the water–air interface. Moreover, irregular aggregation of the Ag nanowires formed at the oil–water interface, because of the slow subsidence of the Ag nanowires, which indicates that the oil–water interface cannot lead to the assembly of Ag nanowires. Therefore, the three-phase interface played a key role in the self-assembly process of the Ag nanowires.

Primary driving forces can explain the self-assembly process of the Ag nanowires in such a three-phase-interface approach. In the first step, the primary driving force for the convective transfer of Ag nanowires was the chloroform evaporation from the oil-air interface. As the chloroform evaporated, the pressure of the oil-air interface decreased, compared to the pressure of the water–oil interface. This pressure gradient ($\Delta P$) produced a mobile phase from the water–oil interface and the bulk oil phase toward the oil-air interface. The mobile phase consisted of chloroform and Ag nanowires. The chloroform compensated for the evaporated chloroform from the oil-air interface, and the Ag nanowires were transferred from the water–oil interface to the water–air interface through the water–air–oil interface. Because of the pressure due to gravity of the water phase, chloroform at the water–oil interface had more fluidity than chloroform in the bulk oil phase. The movement of chloroform at the water–oil interface could drive the transfer of the Ag nanowires at the water–oil phase. Furthermore, although the Ag nanowires could be well dispersed in the water phase, they would slowly subside over a long time. The effect of subsidence of the Ag nanowires could compensate the transferred nanowires at the water–oil interface. Therefore, the smart utility of the interface characterization could spontaneously implement the transfer of the Ag nanowires at the interface without the help of an external force.

In the second step, while more and more Ag nanowires were transferred to the water–air interface, the self-assembly of the Ag nanowires firstly occurred at the contact line of the water phase and the substrate. The same behavior of self-assembly materials at the water–air-substrate interface had been reported by Dimitrov et al.[21] for producing monolayers of spherical polystyrene particles, and by Nikoobakht et al.[3] for the self-assembly of Au nanorods. For example, Nikoobakht et al. used a copper grid as a hard substrate, which was partially inserted into a solution of the Au nanorods, and self-assembly appeared in the vicinity of the water–air–substrate contact line.[3] They proposed that the capillary force was one of the main factors causing the observed self-assembly of the small colloidal particles confined to the thin films. The similarity of our results with those of Dimitrov et al.[21] and Nikoobakht et al.[3] indicate that this similar model can be used to explain the self-assembly of Ag nanowires that initially occurred at the water–air–substrate interface.[3] Therefore, capillary forces might be the main force for the initial self-assembly of the Ag nanowires at the water–air-substrate interface.

In the third step, a film of the Ag nanowires grew from the water–air–substrate interface to the whole water–air interface. Several factors were important in this step. Firstly, Nikoobakht et al.[3] has explained the tendency of nanorods to align side by side rather than end to end, which is mainly due to the higher lateral capillary forces along the length of a nanorod as compared to the width. Furthermore, the theory of capillary interaction between identically sized particles embedded within a thin water film indicates that the capillary interaction between two particles is attractive when the surface of the particles is hydrophilic.[22–24] In our work, for the hydrophilic nanowires, the anisotropy of the interaction between them could be an important driving force for their ordering in a side-by-side alignment. When the nanowires were transferred to the water–air interface, with a hydrophilic surface, lateral capillary forces appeared because of the deformation of the meniscus. The larger the interfacial deformation created by the nanowires, the stronger the capillary forces became between them.[3] As the lateral capillary force drove the side-by-side alignment of the nanowires, the surface tension along the contact line of the solution and a given nanowire and the hydrostatic pressure throughout the nanowire surface decreased, which would further promote the self-assembly of the nanowires.

Furthermore, poly(vinyl pyrrolidone) (PVP) molecules played a key role in the assembly process. Ag nanowires that were prepared by the polyol reduction of $AgNO_3$ in the presence of PVP had very good dispersion in water and poor dispersion in organic solvents due to the protecting layer of PVP on their surface. According to previous reports,[25,26] PVP, as the capping agent, acts on the surface of the Ag nanowires due to strong interactions existing between the carboxyl oxygen atom (C=O) of the PVP and the Ag core surface. Meanwhile, a high-magnification SEM image of the self-assembled Ag nanowires has shown that the protecting layer of the PVP also provides a stronger interaction among the adjacent Ag nanowires, which may improve the nanowires in binding together and aligning parallel to each other (see Supplementary Information, Fig. S2b). The mechanism of formation of the arrays of nanowires needs to be further investigated. In addition, when

PVP molecules were reduced or removed, the self-assembly process could not be achieved due to the poor dispersivity of the Ag nanowires in the water phase. The more times the PVP-capped Ag nanowires were washed, the less ordered the self-assembled film of the Ag nanowires became (see Supplementary Information, Fig. S4). When PVP was replaced with thioglycolic acid, the SEM images showed that the nanowires were partially aggregated with unordered structures (see Supplementary Information, Fig. S4d).

In our experiments, the optimal three phases were water, air, and chloroform. The influence of other solvents has been investigated. When the water phase was replaced with ethanol, the nanowires dispersed in the ethanol could not be assembled, because the ethanol was able to dissolve in the chloroform and no three-phase interface appeared (see Supplementary Information, Fig. S5). Interestingly, Ag nanowires dispersed in a mixed solvent of ethanol and water could assemble, but the SEM image showed that the alignment of the nanowires was not as dense as such assemblies from an aqueous dispersion (see Supplementary Information, Fig. S6).

When the organic solvent was changed from chloroform ($CHCl_3$) to methylene dichloride ($CH_2Cl_2$) or tetrachloromethane ($CCl_4$), similar assembled films could be obtained under the same conditions. Figure 3 shows optical images and the corresponding SEM images of such films after transfer to glass slides. The results demonstrate that the nanowires assemble in the best-ordered and dense form when using chloroform as the oil phase. When $CCl_4$ replaced $CHCl_3$ as the oil phase, nanoparticles, which are by-products of the present synthesis, could cause unequal spacing between the arrays of nanowires and consequently distort the two-dimensional assemblies. However, when using $CH_2Cl_2$ and $CHCl_3$ as the oil phase, the assembly was not influenced by these nanoparticles.

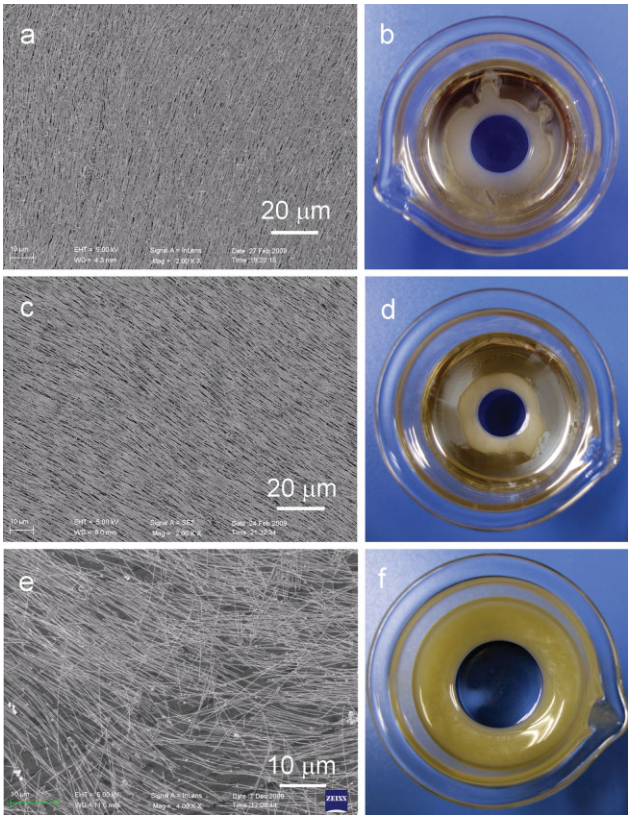


**Figure 3.** SEM images of the films of Ag nanowires and corresponding optical photographs prepared using $CH_2Cl_2$ (a–b), $CHCl_3$ (c–d), and $CCl_4$ (e–f).

The differences in the assembly were probably because of the different saturation vapor pressures and polarities. The saturation vapor pressure is the main factor defining the evaporation properties of the solvents. In our experiments, the evaporation of the oil phase, which caused the transfer of the Ag nanowires from the water–oil interface to the water–air interface, also played an important role in the assembly process. Comparing the saturation vapor pressures (at 298 K) of $CH_2Cl_2$, $CHCl_3$, and $CCl_4$, which are 30.66 kPa, 26.54 kPa, and 15.26 kPa, respectively, $CH_2Cl_2$ and $CHCl_3$ have a higher saturation vapor pressure, and their use resulted in the formation of more-ordered assemblies of Ag nanowires. Moreover, the polarities of $CH_2Cl_2$, $CHCl_3$, $CCl_4$ and water are 3.40, 4.40, 1.60, and 10.20, respectively. The polarity of chloroform is the closest to the polarity of water. In contrast with the other two solvents, chloroform can have more interaction with water, which could favor the assembly process. Therefore, the films of Ag nanowires prepared using $CCl_4$ and $CH_2Cl_2$ were less regular than the film prepared using $CHCl_3$.

Interestingly, self-assembled films of other ultralong nanowires, such as $Ag_6Mo_{10}O_{33}$ and Te nanowires, or $Bi_2S_3$ nanoribbons, can be achieved by using this approach. If the nanowires have no protecting molecules, they should be made with adsorbed PVP molecules, which could help their dispersivity in the water phase and thus aid the self-assembly process. SEM images have shown that $Ag_6Mo_{10}O_{33}$ nanowires with a diameter of 50–60 nm and a length of 100–200 μm can be self-assembled well (Fig. 4a). $Bi_2S_3$ nanoribbons with a width of 200–300 nm and a length of several millimeters could be well aligned parallel to each other, forming ordered assembly films (Fig. 4b). The ultrathin Te nanowires with a diameter of 4–9 nm and a length of 10–20 μm did not self-assemble well and just formed regular alignments on the small, local scale (Fig. 4c). Therefore, compared to ultrathin nanowires, the present approach may be a better fit for the self-assembly of rigid, ultralong nanowires over a large area.

The films with well-aligned Ag nanowires generated some novel optical properties because of the large electromagnetic (EM) fields that were localized in the interstitials of adjacent nanowires. This has great application in the field of ultrasensitive, molecular-specific sensing. Garcia-Vial and Pendry[27] reported that incident radiation can excite surface plasmons trapped in the interstitials between the cylinders, which can generate EM coupling between the aligned silver half-cylinders. In our experiments, the dependence of the UV-vis spectra on the polarization angle of the incident light demonstrates the existence of large EM fields in the films. The polarization angle of the incident light, that is to say, the angle between the polarized electric field and the long axes of the nanowires, was recorded by rotating a half-wave plate in the laser path. When the polarization angle increased from 0° to 90°, the transmission intensity increased. Broadening in the 700–900 nm range was attributed to the coupling of electromagnetic waves among adjacent nanowires (Fig. 5). Yang et al.[5,20] reported that this dependence of the extinction spectra is the result of the dependence of the extinction of longitudinal plasmons within the

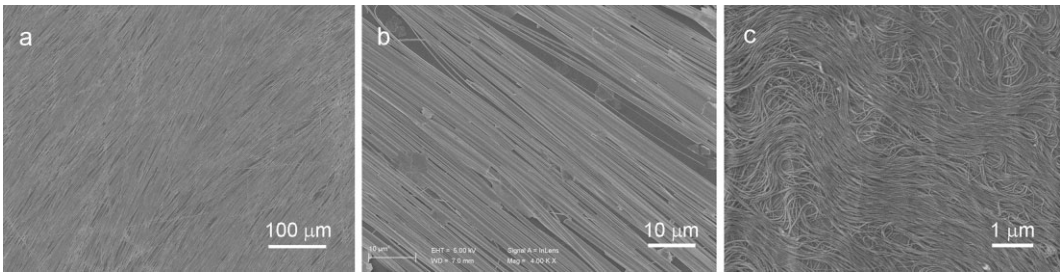


**Figure 4.** a) SEM image of a film of $Ag_6Mo_{10}O_{33}$ nanowires. b) SEM image of a film of $Bi_2S_3$ nanoribbons. c) SEM image of a film of Te nanowires. The films of these nanostructures were made through the three-phase-interface approach.

monolayers. In contrast, for films composed of the randomly distributed Ag nanowires, the transmission intensities showed no change as the polarization angle increased from 0° to 90°. Therefore, the existence of the large EM fields in the film demonstrates the great order of the film of the Ag nanowires.

Importantly, because of the existence of the large EM field, a film of well-aligned Ag nanowires could serve as an excellent surface-enhanced Raman spectroscopy (SERS) substrate for molecular sensing with high sensitivity and selectivity.[5,28–30] In our experiments, we demonstrated the capability of the Ag nanowire films for use in the detection of Rhodamine 6G (R6G) molecules using spontaneous Raman instruments (Fig. 6a). Figure 6b shows the SERS spectra of the R6G molecules (25 μL, $1 \times 10^{-7}$ M) on the Ag nanowire films. When the polarization angle $\theta$ between the polarization direction and the long nanowire axis increased from 0° to 90°, the intensities of the corresponding SERS signals increased. To express this periodicity, we analyzed the typical Raman band (1362 $cm^{-1}$) and plotted a diagram of the SERS intensities and the polarization angle $\theta$ (Fig. 6c). The solid line in Figure 6c is the best fit to a $\cos^2\theta$ function, and is similar to that shown in a previous report.[20]

## 3. Conclusions

In conclusion, we have demonstrated a new and facile way of creating macroscopic, dry, freestanding films of well-aligned Ag nanowires by means of a three-phase-interface self-assembly process. The three-phase interface plays a key role in the process, and could drive the movement and self-assembly of the Ag nanowires. The evaporation of the oil phase, the capillary force, and the PVP molecules are the main factors that promote the self-assembly of ultralong Ag nanowires. A large electromagnetic field existing in the film of the Ag nanowires is observed, implying their potential application as ultrasensitive molecular sensors and optical devices. This three-phase-interface approach has been found to be a general method for the self-assembly of other ultralong inorganic nanowires, and could produce a variety of ordered films of nanowires.

## Experimental

*Chemicals*: All of the reagents (analytical-grade purity) were purchased from Shanghai Chemical Reagents Co. and were used without any further purification.

*Synthesis of the Silver Nanowires*: Uniform Ag nanowires with high aspect ratios were prepared by the polyol process method as reported previously[25,31,32]. Briefly, all of the ethylene glycol (EG) used was refluxed at 196 °C for 5 h to remove trace water. About 10 mL of EG was refluxed in a three-necked round-bottom flask at 160 °C for 1 h. Then, 5 mL of an EG solution of 0.2 M $AgNO_3$ and 5 mL of an EG solution of 0.3 M poly(vinyl pyrrolidone) (PVP) ($M_w = 40\,000$ g $mol^{-1}$) were simultaneously injected into the refluxing solvent, with stirring, at a rate of approximately 0.2 mL $min^{-1}$. The solution turned to opaque gray after about 45 min, indicating the formation of the uniform silver nanowires. The reaction mixture was washed with acetone and centrifuged to remove excess PVP and EG. The washed nanowires were then dispersed in distilled water for the preparation of the following self-assembly.

*Self-Assembly of the Silver Nanowires*: In a typical experiment, about 10 mL of chloroform was added to a glass vessel (we used a glass beaker with a volume of 25 mL and a diameter of 3.5 cm). Then, a certain amount of the aqueous dispersion of silver nanowires was added to the vessel for the creation of the three-phase interface, in which the oil–water–air interface exists at the center of the beaker. After some time, a sparkling film appeared on the whole of the water surface showing that the Ag nanowires were successfully assembled in this process. For the convenient transfer of the film, we slowly added some distilled water in the vicinity of the three-phase interface, making the water phase totally cover the surface of the chloroform. Finally, we could see a sparking film floating on the water surface. The film could be transferred to the desired substrates through the puller system of a Langmuir–Blodgett set-up.

*Synthesis and Self-Assembly of $Ag_6Mo_{10}O_{33}$ Nanowires and $Bi_2S_3$ Nanoribbons*: $Ag_6Mo_{10}O_{33}$ nanowires were prepared following the method previously reported by our group [33]. $Bi_2S_3$ nanoribbons were prepared following the method in a previous report [34]. For the self-assembly of these nanowires, we needed to make the PVP molecules adsorb on the surface of the nanowires. Firstly, an amount of PVP molecules was added to the nanowire solution; then, the solution was stirred for one day at room temperature. Finally, the nanowires were washed with distilled water and dispersed in distilled water.

*Synthesis and Self-Assembly of Ultrathin Te Nanowires*: The Te nanowires were prepared following the method previously reported by our group [35]. Because the as-synthesized Te nanowires had been stabilized by PVP molecules, these nanowires could be directly self-assembled without further treatment.

*Preparation of SERS Samples*: The self-assembled silver nanowire films were transferred to 10 mm × 10 mm glass slides, and dried naturally. Then, 25 μL of R6G ($1 \times 10^{-7}$ M) was added slowly and dried for the SERS measurements.

*Characterization*: Field-emission SEM (FESEM) was applied to investigate the size and morphology of the nanowires, and was carried out using a field-emission scanning electron microanalyzer (JEOL-6700F and ZEISS SUPRA 40). X-Ray powder diffraction was carried out using a Rigaku Dmax-γA X-ray diffractometer, and the morphologies of the as-prepared products were observed by transmission electron microscopy (JEOL-2010). High-resolution transmission electron microscopy photos were taken using a

JEOL-2010 transmission electron microscope. The UV-vis transmission spectra were obtained using a near-field microscope. All of the Raman experimental data were obtained using a continuous-wave (cw) laser source (Coherent, Verdi-5W, 532 nm) and a triple-grating monochromator coupled to a liquid-nitrogen-cooled CCD detector (Acton Research, TriplePro). The precision of the spectral measurements with this monochromator was estimated by the mercury spectral lines to be better than 0.01 $cm^{-1}$. A 90° Raman scattering geometry was employed.

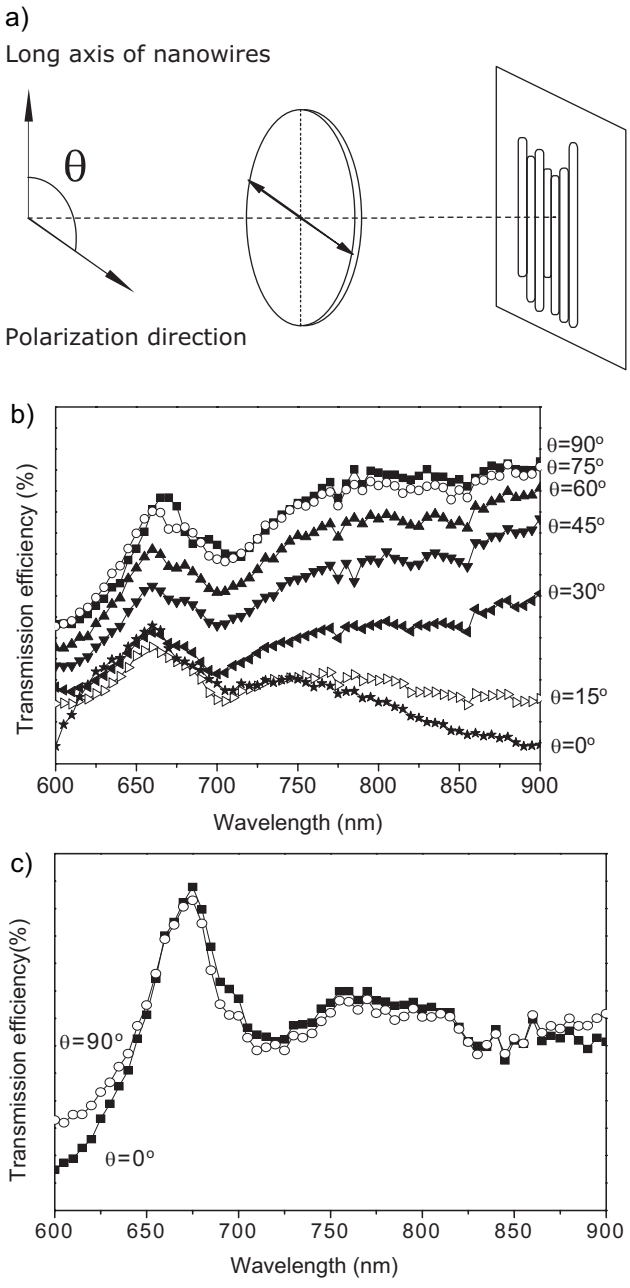


**Figure 5.** a) Schematic illustration of the polarization angle $\theta$, which is defined as the angle between the polarization direction and the long nanowire axis. b) UV-vis transmission spectra of the film of silver nanowires. All of the spectra were obtained at normal incidence with polarization angles ($\theta$) in the range of 0–90°. c) UV-vis transmission spectra of the film made by the randomly dispersed Ag nanowires. The spectra are obtained at polarization angles ($\theta$) of 0° (dot) and 90° (square), respectively.

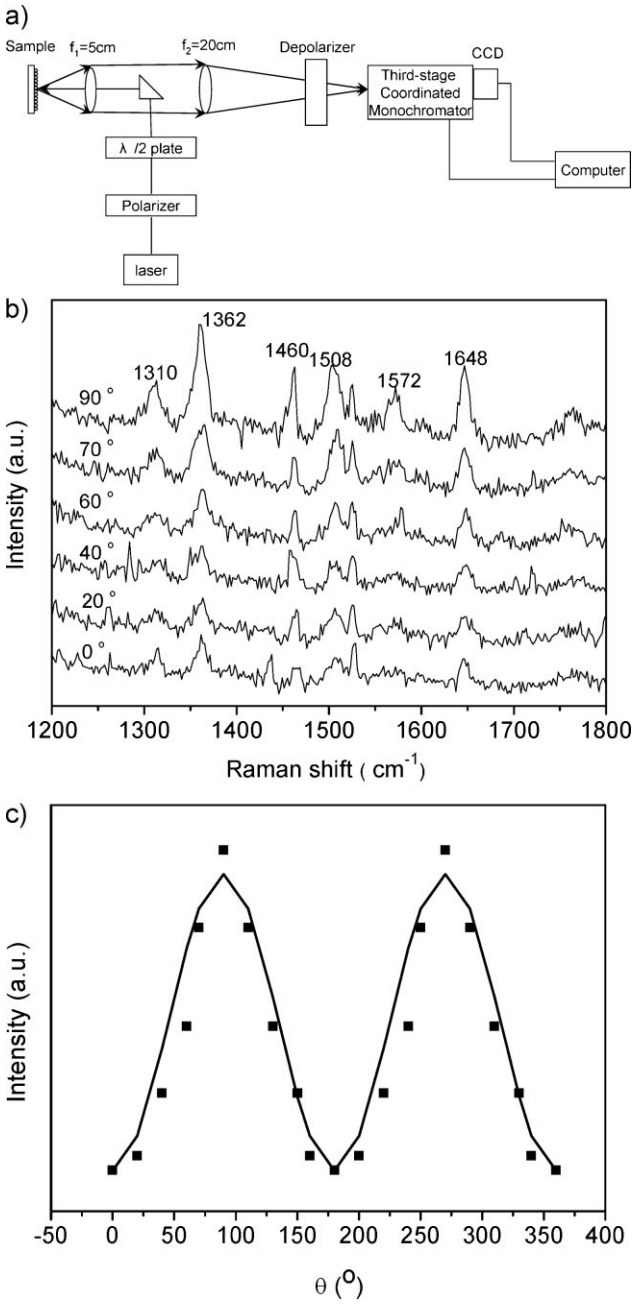


**Figure 6.** a) Schematic illustration showing the spontaneous Raman scattering instruments used for the 180° backscattered SERS experiments. b) SERS spectra of adsorbed Rhodamine 6G (25 μL, $1 \times 10^{-7}$ M) on a film taken at different polarization directions of incident light. c) The line represents the best fit to a periodic cosine function; the square dots represent the relationship between the polarization angle and the SERS intensities of the peak at 1362 $cm^{-1}$.

## Acknowledgements

We acknowledge the funding support from the National Basic Research Program of China (2010CB934700), the Program of International S & T Cooperation (S2010GR0314), the National Science Foundation of China (Grant Nos. 50732006, 20671085), and the Partner Group of the Chinese Academy of Sciences and the Max Planck Society. Hong-Yan Shi and Bo Hu contributed equally to this work. Supporting Information is available online from Wiley InterScience or from the author.

Received: September 5, 2009
Published online: March 4, 2010

[1] Y. N. Xia, P. D. Yang, Y. G. Sun, Y. Y. Wu, B. Mayers, B. Gates, Y. D. Yin, F. Kim, Y. Q. Yan, *Adv. Mater.* **2003**, *15*, 353.
[2] S. J. Guo, S. J. Dong, E. K. Wang, *Cryst. Growth Des.* **2009**, *9*, 372.
[3] B. Nikoobakht, Z. L. Wang, M. A. El-Sayed, *J. Phys. Chem. B* **2000**, *104*, 8635.
[4] H. Shimoda, S. J. Oh, H. Z. Geng, R. J. Walker, X. B. Zhang, L. E. McNeil, O. Zhou, *Adv. Mater.* **2002**, *14*, 899.
[5] A. Tao, F. Kim, C. Hess, J. Goldberger, R. R. He, Y. G. Sun, Y. N. Xia, P. D. Yang, *Nano Lett.* **2003**, *3*, 1229.
[6] J. Matsui, K. Yamamoto, N. Inokuma, H. Orikasa, T. Kyotani, T. Miyashita, *J. Mater. Chem.* **2007**, *17*, 3806.
[7] Y. Lin, A. Boker, H. Skaff, D. Cookson, A. D. Dinsmore, T. Emrick, T. P. Russell, *Langmuir* **2005**, *21*, 191.
[8] N. Glaser, D. J. Adams, A. Boker, G. Krausch, *Langmuir* **2006**, *22*, 5227.
[9] A. Boker, Y. Lin, K. Chiapperini, R. Horowitz, M. Thompson, V. Carreon, T. Xu, C. Abetz, H. Skaff, A. D. Dinsmore, T. Emrick, T. P. Russell, *Nat. Mater.* **2004**, *3*, 302.
[10] S. Biswas, L. T. Drzal, *Nano Lett.* **2009**, *9*, 167.
[11] J. He, Q. Zhang, S. Gupta, T. Emrick, T. R. Russell, P. Thiyagarajan, *Small* **2007**, *3*, 1214.
[12] Y. K. Park, S. H. Yoo, S. Park, *Langmuir* **2007**, *23*, 10505.
[13] A. Kulak, Y. J. Lee, Y. S. Park, H. S. Kim, G. S. Lee, K. B. Yoon, *Adv. Mater.* **2002**, *14*, 526.
[14] Y. J. Min, M. Akbulut, K. Kristiansen, Y. Golan, J. Israelachvili, *Nat. Mater.* **2008**, *7*, 527.
[15] Y. Bae, N. H. Kim, M. Kim, K. Y. Lee, S. W. Han, *J. Am. Chem. Soc.* **2008**, *130*, 5432.
[16] S. H. Im, Y. T. Lim, D. J. Suh, O. O. Park, *Adv. Mater.* **2002**, *14*, 1367.
[17] K. Ariga, J. P. Hill, M. V. Lee, A. Vinu, R. Charvet, S. Acharya, *Sci. Technol. Adv. Mater.* **2008**, *9*, 014109.
[18] F. Westerlund, T. Bjornholm, *Curr. Opin. Colloid Interface Sci.* **2009**, *14*, 126.
[19] I. Patla, S. Acharya, L. Zeiri, J. Israelachvili, S. Efrima, Y. Golan, *Nano Lett.* **2007**, *7*, 1459.
[20] A. R. Tao, P. D. Yang, *J. Phys. Chem. B* **2005**, *109*, 15687.
[21] A. S. Dimitrov, K. Nagayama, *Langmuir* **1996**, *12*, 1303.
[22] P. A. Kralchevsky, V. N. Paunov, I. B. Ivanov, K. Nagayama, *J. Colloid Interface Sci.* **1992**, *151*, 79.
[23] K. P. Velikov, F. Durst, O. D. Velev, *Langmuir* **1998**, *14*, 1148.
[24] H. Xia, D. Wang, *Adv. Mater.* **2008**, *20*, 4253.
[25] P. Jiang, S. Y. Li, S. S. Xie, Y. Gao, L. Song, *Chem. Eur. J.* **2004**, *10*, 4817.
[26] Y. Gao, P. Jiang, D. F. Liu, H. J. Yuan, X. Q. Yan, Z. P. Zhou, J. X. Wang, L. Song, L. F. Liu, W. Y. Zhou, G. Wang, C. Y. Wang, S. S. Xie, J. M. Zhang, A. Y. Shen, *J. Phys. Chem. B* **2004**, *108*, 12877.
[27] F. J. GarciaVidal, J. B. Pendry, *Phys. Rev. Lett.* **1996**, *77*, 1163.
[28] J. P. Kottmann, O. J. F. Martin, *Opt. Express* **2001**, *8*, 655.
[29] J. P. Kottmann, O. J. F. Martin, D. R. Smith, S. Schultz, *Chem. Phys. Lett.* **2001**, *341*, 1.
[30] J. P. Kottmann, O. J. F. Martin, D. R. Smith, S. Schultz, *Phys. Rev. B: Condens. Matter* **2001**, *64*.
[31] Y. G. Sun, Y. N. Xia, *Adv. Mater.* **2002**, *14*, 833.
[32] Y. G. Sun, Y. D. Yin, B. T. Mayers, T. Herricks, Y. N. Xia, *Chem. Mater.* **2002**, *14*, 4736.
[33] X. J. Cui, S. H. Yu, L. L. Li, L. Biao, H. B. Li, M. S. Mo, X. M. Liu, *Chem. Eur. J.* **2004**, *10*, 218.
[34] Z. P. Liu, S. Peng, Q. Xie, Z. K. Hu, Y. Yang, S. Y. Zhang, Y. T. Qian, *Adv. Mater.* **2003**, *15*, 936.
[35] H. S. Qian, S. H. Yu, J. Y. Gong, L. B. Luo, L. F. Fei, *Langmuir* **2006**, *22*, 3830.